Nonequilibrium Green functions depending on the observation time for ultrafast dynamics

Mamoru Sakaue* and Toshiaki Munakata
RIKEN (The Institute of Physical and Chemical Research), Wako, Saitama 351-0198, Japan

Hideaki Kasai†
Department of Applied Physics, Osaka University, Suita, Osaka 565-0871, Japan

Ayao Okiji
Wakayama National College of Technology, Nada, Gobo, Wakayama 644-0023, Japan
(Received 7 May 2002; published 12 September 2002)

Nonequilibrium Green functions depending on the observation time are introduced in order to investigate ultrafast dynamics involved in photoemission from metal surfaces. Phase decay due to scattering of secondary particles (electrons and holes in the metal) accounts for the dependence of the Green functions on the observation time of a main particle (photoelectron) in the final state. The Green functions G^{+-} and G^{-+} striding over the forward and backward branches of the Keldysh contour represent the dynamics of the secondary particles, i.e., decay of the secondary particles and electron thermalization due to inelastic scattering of the secondary particles. Then, by applying the Green functions to two-photon photoemission from a metal surface, it is shown that the decay of photoexcited holes accelerates the decrease of the photoelectron intensity as a function of the pump-probe delay time and the electron thermalization can account for dephasing.

DOI: 10.1103/PhysRevB.66.094302 PACS number(s): 71.10.−w, 05.30.−d, 78.68.+m, 79.60.−i

I. INTRODUCTION

Owing to the recent progress in the femtosecond laser technology, investigation of laser-induced coherent processes in solids as well as atoms and molecules in the gas phase has become an absorbing topic of physics and chemistry. Especially, electron dynamics at noble-metal surfaces is one of the ideal subjects for investigating quantum dynamics of coherently excited quasiparticles since the electronic structures of the metals are well known[1,2] and experimental techniques for controlling interactions involving surface states, defects, and adsorbates of the metals are well investigated.[3]

Here we focus on the time-resolved two-photon photoemission (time-resolved 2PPE, TR2PPE) spectroscopy on the surfaces.[3–6] In a simple model, first an electron in an occupied state is excited to an unoccupied state by a pump-laser pulse. Then electron relaxation (decrease of the electron density) and dephasing (decrease of the electron polarization) can begin because of electron-electron/electron-phonon scattering, or electron scattering by local potentials around defects, impurities, and the surface. Subsequently, the electron is excited to a free-electron state above the vacuum level by a probe-laser pulse and hence emitted from the surface.

The 2PPE spectra are measured as functions of the pump-probe delay time and then information on the transient behavior of the system affected by relaxation and dephasing can be obtained. Estimation of both the electron lifetimes and dephasing times from the TR2PPE spectra has been attempted by phenomenological analysis with the aid of optical Bloch equations.[3,5] Although microscopic mechanisms of electron relaxation have been extensively studied by quantitative calculation of the lifetimes of the electron states,[2,7,8] microscopic analysis of the dephasing times is still an unresolved issue.

For analysis of experimental TR2PPE spectra, usually, the photoelectron densities are calculated based on optical Bloch equations.[3,5] Originally, basic theories regarding optical Bloch equations are formulated for quantum optics of atoms and molecules in the gas phase.[9] Electrons in the atoms and molecules can interact with the electromagnetic field and hence recombine with holes by spontaneous emission. The lifetime of the electronically excited state due to this mechanism is defined to be an energy relaxation time τ_1. When the atoms and molecules collide with each other, the quantum phase of the electron system can change. Both the spontaneous emission and the collision accounts for phase decay of which the time scale can be given by a dephasing time $\tau_2 = (1/2\tau_1 + 1/\overline{\tau_2})^{-1}$, where $\overline{\tau_2}$ is a pure dephasing time due to elastic scattering between the atoms and molecules. Quantum optics of insulators and semiconductors is similar to that of atoms and molecules in the gas phase except that electron-phonon interactions and electron scattering at local potentials around defects, impurities, and surfaces account for dephasing instead of the collisions.[10]

One might apply the above theory to quantum optics at metal surfaces.[11] For example, we assume that a partial system consists of occupied and unoccupied surface states. Photoexcited electrons and holes can relax due to inelastic scattering by other electrons in the metal. The lifetime of a photoexcited electron is usually taken into account in optical Bloch equations by assuming that τ_1 corresponds to the lifetime. Although mechanisms of dephasing at metal surfaces have not been clarified yet, phenomenological dephasing times $\overline{\tau_2}$ are taken into account by analogy of the quantum optics of insulators and semiconductors.[3,5]

However, mechanisms of relaxation and dephasing at metal surfaces should be different from those of insulators and semiconductors because of existence of the Fermi surface. By inelastic electron-electron scattering of photoexcited

electrons and holes, secondary electrons and holes can be excited in the vicinity of the Fermi level.[12] These secondary electrons and holes can be inelastically scattered again and hence dissipate into the metal by losing coherence (thermalization). Therefore we can deduce that *microscopically* inelastic scattering can account for *macroscopically* elastic scattering introduced within the framework of optical Bloch equations. Then the observation probability of the photoelectron, i.e., the photoelectron density, can change dynamically until the observation because of the phase decay due to scattering of the secondary electrons and holes which remain in the metal after the photoemission (here, photoexcited holes can be classified as secondary particles since the relaxation processes of the electrons and holes in metals are usually independent of each other). Thus the observation time dependence of the photoelectron density contains information on the phase decay. However, as shown in Sec. III, the observation time dependence cannot be derived from optical Bloch equations. Therefore it is necessary to introduce another method by which we can investigate the effects of scattering of the secondary electrons and holes on the observation time dependence.

Green functions are useful tools for investigation of electron dynamics from a microscopic point of view. Especially the Keldysh Green-function method[13,14] is one of the representative methods for investigating nonequilibrium problems including photoemission. However this method is not effective for investigating the observation time dependence since the Green functions are defined by assuming efficiently long observation times. In this paper, we introduce nonequilibrium Green functions for finite observation times by perturbative expansion of a density matrix. Then we discuss on the basis of the formulas of the Green functions how the dynamics of the secondary electrons and holes is concerned with the observation time dependence of the Green functions. By applying these Green functions to 2PPE from a metal surface, we demonstrate how the photoexcited hole decay and thermalization of secondary electrons and holes affect the photoelectron density.

In fact, absolute-time dependence of the Keldysh Green functions is an important issue of many-body quantum theory. The original theory by Keldysh[13] suggests nothing about the absolute-time dependence so the correlation functions in the Green functions may be given by the spectral theorem in the same way as the equilibrium Green functions. By the Keldysh rotation, the Keldysh Green functions are transformed into advanced and retarded Green functions and a ''dynamical distribution function.'' By deducing from semiclassical theories, some ideas were proposed that the dynamical distribution function will depend on the absolute times when the state of the system is far from the equilibrium.[14,15] Then the absolute-time dependence of the dynamical distribution function can be introduced by attaching additional conditions based on these hypotheses, e.g., the generalized Kadanoff-Baym ansatz.[15] Although there are applications of the Green functions based on the hypotheses to dynamics induced by ultrashort laser pulses,[16,17] the requirement of the hypotheses in which the quantum theoretical basis is not solid makes the Keldysh Green-function method inconvenient and, in numerous cases, the absolute-time dependence is ignored for simplicity.[18–22] By taking an example of one-photon photoemission (1PPE) spectroscopy which can probe the hole dynamics in the energy domain,[18–25] we discuss this problem by referring to the results obtained by the Green-function method introduced in this paper.

II. NONEQUILIBRIUM GREEN FUNCTIONS

We introduce a system of which the Hamiltonian is described as $H=H_0+H'(t)$, where the unperturbed Hamiltonian is given by

$$H_0=\sum_{\mu} E_{\mu}c_{\mu}^{\dagger}c_{\mu}. \tag{1}$$

Here E_{μ}, $c_{\mu}^{\dagger}$, and c_{μ} stand for the energy and the creation and annihilation operators of a quantum state (including a spin) $|\mu\rangle$ of a particle, respectively. The perturbation $H'(t)=W(t)+V$ consists of interactions of a particle with time-dependent external fields,

$$W(t)=\sum_{\mu,\nu} W_{\mu\nu}(t)c_{\mu}^{\dagger}c_{\nu}, \tag{2}$$

and two-body interactions between the particles,

$$V=\frac{1}{2}\sum_{\kappa,\lambda,\mu,\nu} V_{\kappa\lambda/\mu\nu}c_{\lambda}^{\dagger}c_{\kappa}^{\dagger}c_{\mu}c_{\nu}. \tag{3}$$

The density matrix of the whole system can be expanded with respect to $H'(t)$ as[26]

$$\begin{aligned}
\rho_{\mu\nu}(t_{\mathrm{ob}}) &= \frac{\mathrm{Tr}[\rho(t_{\mathrm{ob}})c_{\nu}^{\dagger}c_{\mu}]}{\mathrm{Tr}[\rho(t_{\mathrm{ob}})]} \\
&= \sum_{n=0}^{\infty}\sum_{n'=0}^{\infty}\left(\frac{1}{i\hbar}\right)^{n+n'}\int_{\infty}^{-\infty}\mathrm{d}t_1'\ldots\int_{\infty}^{-\infty}\mathrm{d}t_{n'}' \\
&\quad\times\int_{-\infty}^{\infty}\mathrm{d}t_n\ldots\int_{-\infty}^{\infty}\mathrm{d}t_1\,\theta(t_{\mathrm{ob}}-t_{n'}') \\
&\quad\times\theta(t_{n'}'-t_{n'-1}')\ldots\theta(t_2'-t_1')\theta(t_1'-t_0) \\
&\quad\times\theta(t_{\mathrm{ob}}-t_n)\theta(t_n-t_{n-1})\ldots\theta(t_2-t_1)\theta(t_1-t_0) \\
&\quad\times\langle h'(t_1')\ldots h'(t_{n'-1}')h'(t_{n'}')c_{\nu}^{\dagger}(t_{\mathrm{ob}}) \\
&\quad\times c_{\mu}(t_{\mathrm{ob}})h'(t_n)h'(t_{n-1})\ldots h'(t_1)\rangle \\
&\equiv \sum_{n=0}^{\infty}\left(\frac{1}{i\hbar}\right)^{n}\frac{1}{n!}\int_{-\infty}^{\infty}\mathrm{d}t_1\ldots\int_{-\infty}^{\infty}\mathrm{d}t_n \\
&\quad\times\langle \mathrm{T}_c(t_{\mathrm{ob}})[c_{\nu}^{\dagger}(t_{\mathrm{ob}}^{-})c_{\mu}(t_{\mathrm{ob}}^{+})h'(t_1)\ldots h'(t_n)]\rangle,
\end{aligned} \tag{4}$$

where $\theta(t)$ is a step function, and

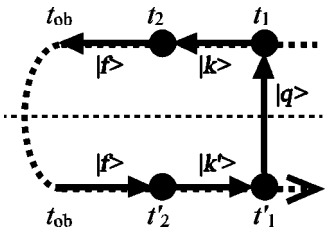

FIG. 1. Example of a fourth-order diagram with respect to interactions W of a particle (fermion) with external fields. A dotted arrow denotes the Keldysh contour where W denoted by dots are ordered as t_1, t_2, t_2', and t_1'. The horizontal dashed line divides the diagram into the forward branch (upper side) and the backward branch (lower side). Solid arrows denote one-particle Green functions for quantum states indicated by appended wave vectors.

$$\langle A\rangle = \frac{\mathrm{Tr}[\rho_0(t_0)A]}{\mathrm{Tr}[\rho_0(t_{\mathrm{ob}})]} \tag{5}$$

stands for the statistical average $\{\mathrm{Tr}[\rho_0(t)]=\mathrm{Tr}[\rho(t)]$ is independent of $t\}$ of an operator A. t_0 is the time at which the system is in the equilibrium state and we can give $t_0\to-\infty$. Here $c_\mu^\dagger(t)$, $c_\mu(t)$, $\rho_0(t)$, and $h'(t)=w(t)+v(t)$ are $c_\mu^\dagger$, c_μ, $\rho(t)$ and $H'(t)$ in the interaction representation, respectively. From Eq. (4), we obtain $\rho_0(t_0)=\exp(-H_0/k_{\mathrm{B}}T)$, where k_{B} is the Boltzmann constant and T is the temperature. $T_c(t_{\mathrm{ob}})[\ \dots\ ]$ denotes that the contained operators are ordered along the Keldysh contour[13,14,27] where the time evolves first from t_1, to the observation time t_{ob} (forward branch), and next from t_{ob} to t_1' (backward branch).

We consider an example of 2PPE from a metal surface that a fermion in an interacting system (electron in a metal) is consecutively excited by external fields (ultraviolet and visible laser pulses) twice before detection by an instrument at t_{ob} as given by a diagram in Fig. 1. Here, first a particle in $|q\rangle$ is excited to $|k\rangle$ (forward branch) or $|k'\rangle$ (backward branch), and subsequently the particle is excited to $|f\rangle$. Then we obtain the density of $|f\rangle$ as

$$\begin{aligned}\rho_{ff}(t_{\mathrm{ob}}) = -i\hbar \lim_{t\to t_{\mathrm{ob}}-0}\lim_{t'\to t_{\mathrm{ob}}-0}\sum_k\sum_{k'}\sum_q \int_\infty^{-\infty} dt_1' \\ \times\int_\infty^{-\infty} dt_2'\int_{-\infty}^{\infty} dt_2\int_{-\infty}^{\infty} dt_1\,\theta(t_{\mathrm{ob}}-t_2') \\ \times\theta(t_2'-t_1')\,\theta(t_{\mathrm{ob}}-t_2)\,\theta(t_2-t_1)W_{qk'}(t_1') \\ \times W_{k'f}(t_2')W_{fk}(t_2)W_{kq}(t_1)G_{ff}^{++}(t,t_2;t_{\mathrm{ob}}) \\ \times G_{kk}^{++}(t_2,t_1;t_{\mathrm{ob}})G_{qq}^{+-}(t_1,t_1';t_{\mathrm{ob}}) \\ \times G_{k'k'}^{--}(t_1',t_2';t_{\mathrm{ob}})G_{ff}^{--}(t_2',t';t_{\mathrm{ob}}).\end{aligned} \tag{6}$$

Here we introduce the *intrabranch* Green functions by

$$\begin{aligned}G_{\mu\nu}^{++}(t,t';t_{\mathrm{ob}}) &= [G_{\nu\mu}^{--}(t',t;t_{\mathrm{ob}})]^* \\ &= \sum_{n=0}^{\infty}\sum_{n'=0}^{\infty}\left(\frac{1}{i\hbar}\right)^{n+n'+1}\int_\infty^{-\infty} dt_1'\dots\int_\infty^{-\infty} dt_{n'}'\int_{-\infty}^{\infty} dt_n\dots\int_{-\infty}^{\infty} dt_1\,\theta(t_{\mathrm{ob}}-t_{n'}')\dots\theta(t_2'-t_1') \\ &\times\theta(t_{\mathrm{ob}}-t_n)\dots\theta(t_2-t_1)\sum_{l=1}^{n}\sum_{l'=1}^{n}\theta(t_{l+1}-t)\,\theta(t-t_l)\,\theta(t_{l'+1}-t')\,\theta(t'-t_{l'}) \\ &\times[\,\theta(t-t')\langle v(t_1')\dots v(t_{n'}')v(t_n)\dots c_\mu(t)\dots c_\nu^\dagger(t')\dots v(t_1)\rangle \\ &\mp\theta(t'-t)\langle v(t_1')\dots v(t_{n'}')v(t_n)\dots c_\nu^\dagger(t')\dots c_\mu(t)\dots v(t_1)\rangle],\end{aligned} \tag{7}$$

and the *interbranch* Green function by

$$\begin{aligned}G_{\mu\nu}^{+-}(t,t';t_{\mathrm{ob}}) &= \mp\sum_{n=0}^{\infty}\sum_{n'=0}^{\infty}\left(\frac{1}{i\hbar}\right)^{n+n'+1}\int_\infty^{-\infty} dt_1'\dots\int_\infty^{-\infty} dt_{n'}' \\ &\times\int_{-\infty}^{\infty} dt_n\dots\int_{-\infty}^{\infty} dt_1\,\theta(t_{\mathrm{ob}}-t_{n'}')\dots\theta(t_2'-t_1') \\ &\times\theta(t_{\mathrm{ob}}-t_n)\dots\theta(t_2-t_1)\sum_{l=1}^{n}\sum_{l'=1}^{n'}\theta(t_{l+1}-t) \\ &\times\theta(t-t_l)\,\theta(t_{l'+1}'-t')\,\theta(t'-t_{l'}') \\ &\times\langle v(t_1')\dots c_\nu^\dagger(t')\dots v(t_{n'}') \\ &\times v(t_n)\dots c_\mu(t)\dots v(t_1)\rangle,\end{aligned} \tag{8}$$

where t_{n+1} and $t'_{n'+1}$ in the summations are replaced with t_{ob}. The functions for fermions take the upper signs and those for bosons take the lower signs. We can also introduce another interbranch Green function by deriving a formula of the hole density for a diagram in which the bold arrows in Fig. 1 are reversed:

$$G^{-+}_{\mu\nu}(t,t';t_{\rm ob})$$
$$=\sum_{n=0}^{\infty}\sum_{n'=0}^{\infty}\left(\frac{1}{i\hbar}\right)^{n+n'+1}\int_{\infty}^{-\infty}dt'_1\ldots\int_{\infty}^{-\infty}dt'_{n'}$$
$$\times\int_{-\infty}^{\infty}dt_n\ldots\int_{-\infty}^{\infty}dt_1\,\theta(t_{\rm ob}-t'_{n'})\ldots\theta(t'_2-t'_1)$$
$$\times\theta(t_{\rm ob}-t_n)\ldots\theta(t_2-t_1)\sum_{l=1}^{n}\sum_{l'=1}^{n'}\theta(t'_{l'+1}-t)$$
$$\times\theta(t-t'_{l'})\theta(t_{l+1}-t')\theta(t'-t_l)\langle v(t'_1)\ldots c_\mu(t)\ldots$$
$$\times v(t'_{n'})v(t_n)\ldots c^{\dagger}_{\nu}(t')\ldots v(t_1)\rangle. \quad (9)$$

Equations (7)–(9) can be rewritten by using the time-ordering symbol as

$$G^{AB}_{\mu\nu}(t,t';t_{\rm ob})=\sum_{n=0}^{\infty}\left(\frac{1}{i\hbar}\right)^{n}\frac{1}{n!}\int_{-\infty}^{\infty}dt_1\ldots\int_{-\infty}^{\infty}dt_n$$
$$\times\langle T_c(t_{\rm ob})[c_\mu(t^A)c^{\dagger}_{\nu}(t'^B)v(t_1)\ldots v(t_n)]\rangle, \quad (10)$$

where A and B are '+' or '−'. These Green functions satisfy the equation of motion in the matrix representation in the same way as do the usual Keldysh Green functions:[14]

$$\left[i\hbar\frac{\partial}{\partial t}-H_0\right]\boldsymbol{\sigma}_z\boldsymbol{G}(t,t';t_{\rm ob})-\int_{-\infty}^{\infty}dt''\,\boldsymbol{\Sigma}(t,t'';t_{\rm ob})\boldsymbol{G}(t'',t';t_{\rm ob})$$
$$=\delta(t-t')\boldsymbol{I}, \quad (11)$$

where

$$\boldsymbol{G}(t,t';t_{\rm ob})=\begin{pmatrix}G^{++}(t,t';t_{\rm ob}) & G^{+-}(t,t';t_{\rm ob})\\ G^{-+}(t,t';t_{\rm ob}) & G^{--}(t,t';t_{\rm ob})\end{pmatrix}, \quad (12)$$

$$\boldsymbol{\Sigma}(t,t';t_{\rm ob})=\begin{pmatrix}\Sigma^{++}(t,t';t_{\rm ob}) & \Sigma^{+-}(t,t';t_{\rm ob})\\ \Sigma^{-+}(t,t';t_{\rm ob}) & \Sigma^{--}(t,t';t_{\rm ob})\end{pmatrix}, \quad (13)$$

$$\boldsymbol{\sigma}_z=\begin{pmatrix}1 & 0\\ 0 & -1\end{pmatrix}, \quad (14)$$

$$\boldsymbol{I}=\begin{pmatrix}1 & 0\\ 0 & 1\end{pmatrix}. \quad (15)$$

Here the self-energy functions are given by

$$\Sigma^{AB}_{\mu\nu}(t,t';t_{\rm ob})$$
$$=\sum_{n=0}^{\infty}\left(\frac{1}{i\hbar}\right)^{n}\frac{1}{n!}\int_{-\infty}^{\infty}dt_1\ldots\int_{-\infty}^{\infty}dt_n\Bigg\{2^{-1}(n_A+n_B)$$
$$\times\sum_{\alpha\beta}[V_{\alpha\mu/\beta\nu}\mp V_{\alpha\mu/\nu\beta}]\langle T_c(t_{\rm ob})[c^{\dagger}_{\alpha}(t^A+n_A\eta)c_\beta(t^A)$$
$$\times v(t_1)\ldots v(t_n)]\rangle+n_An_B\sum_{\alpha\beta\gamma}\sum_{\alpha'\beta'\gamma'}V_{\alpha\mu/\beta\gamma}$$

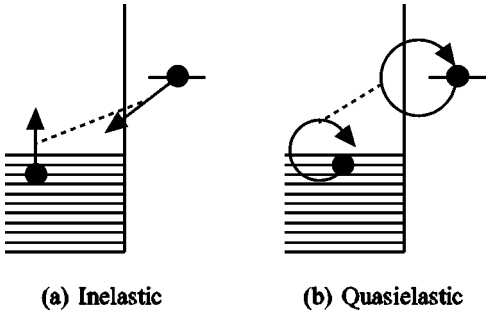

FIG. 2. Examples of (a) inelastic and (b) quasielastic scattering involving homogeneous and inhomogeneous fermion states. Left sides show the energy diagram of initially occupied homogeneous states in the shaded areas and unoccupied states in the empty areas. Right sides show the energy level of an inhomogeneous state occupied by a main particle which is to be scattered. Dashed lines denote interactions between particles indicated by filled circles.

$$\times V_{\gamma'\beta'/\nu\alpha}\langle T_c(t_{\rm ob})[c^{\dagger}_{\alpha}(t^A+2n_A\eta)c_\beta(t^A+n_A\eta)c_\gamma(t^A)$$
$$\times c^{\dagger}_{\gamma'}(t'^B+2n_B\eta)c^{\dagger}_{\beta'}(t'^B+n_B\eta)$$
$$\times c_{\alpha'}(t'^B)v(t_1)\ldots v(t_n)]\rangle\Bigg\}, \quad (16)$$

where A and B are '+' or '−', $n_+=1$ and $n_-=-1$, and $\eta\to+0$. Diagrammatic expansion of the correlation functions in Eqs. (7)−(9) and (16) is possible by Wick's theorem (or Bloch–de Dominicis's theorem) in the same way as the expansion of correlation functions included in the usual Keldysh Green functions.[14]

It is useful to write the intrabranch Green functions in Eq. (7) as functions of the absolute time t of which the origin is $t_{\rm ob}$ as well as functions of the relative time $t-t'$:

$$G^{++}_{\mu\nu}(t,t';t_{\rm ob})=G^{++}_{\mu\nu}(t_{\rm ob}-t,t-t'), \quad (17)$$

$$G^{--}_{\nu\mu}(t,t';t_{\rm ob})=G^{--}_{\nu\mu}(t-t',t'-t_{\rm ob}). \quad (18)$$

Here the signs of the relative times are defined by referring to the time ordering along the Keldysh contour. In case of $t>t'$ in $G^{++}(t,t';t_{\rm ob})$, for example, after excitation of a main particle at t', the particle can be scattered inelastically until t [see Fig. 2(a)]. Thus the $t-t'$ dependence of the intrabranch Green functions mainly represents the relaxation of the main particle (e.g., electrons in $|k\rangle$, $|k'\rangle$, and $|f\rangle$) in the same way as do the usual Green functions. The main particle can also be scattered quasielastically from t' to t so that secondary particles are excited [see Fig. 2(b)].[28] The secondary particles can be scattered before the observation of the main particle at $t_{\rm ob}$. Thus the $t_{\rm ob}-t$ dependence of the intrabranch Green functions represents the dephasing due to quasielastic scattering. When the quasielastic scattering is negligible, the intrabranch Green functions become independent of $t_{\rm ob}$ and hence equivalent to the usual Green functions $G^{++}(t-t')$ and $G^{--}(t-t')$.

It is useful to write the interbranch Green functions in Eqs. (8) and (9) as functions of the absolute times t and t' of which the origin is $t_{\rm ob}$:

$$G^{+-}_{\mu\nu}(t,t';t_{\rm ob})=G^{+-}_{\mu\nu}(t_{\rm ob}-t,t'-t_{\rm ob}), \quad (19)$$

$$G_{\mu\nu}^{-+}(t,t';t_{\rm ob})=G_{\mu\nu}^{-+}(t-t_{\rm ob},t_{\rm ob}-t'). \tag{20}$$

These functions mainly represent the relaxation of secondary particles (e.g., hole in $|q\rangle$) which are excited at t and t' in the forward and backward branches, respectively, and scattered before the observation of the main particle at $t_{\rm ob}$. By expanding Dyson's equations derived from Eq. (11), $G_{\mu\nu}^{+-}(t,t';t_{\rm ob})$ and $G_{\mu\nu}^{-+}(t,t';t_{\rm ob})$ can be divided into two terms:

$$G_{\mu\nu}^{+-}(t,t';t_{\rm ob})=G_{\mu\nu}^{+-\,[1]}(t,t';t_{\rm ob})+G_{\mu\nu}^{+-\,[2]}(t,t';t_{\rm ob}), \tag{21}$$

$$G_{\mu\nu}^{-+}(t,t';t_{\rm ob})=G_{\mu\nu}^{-+\,[1]}(t,t';t_{\rm ob})+G_{\mu\nu}^{-+\,[2]}(t,t';t_{\rm ob}). \tag{22}$$

Here, as shown in the following, $G_{\mu\nu}^{+-\,[1]}(t,t';t_{\rm ob})$ and $G_{\mu\nu}^{-+\,[1]}(t,t';t_{\rm ob})$ represent decay of a secondary particle, and $G_{\mu\nu}^{+-\,[2]}(t,t';t_{\rm ob})$ and $G_{\mu\nu}^{-+\,[2]}(t,t';t_{\rm ob})$ represent thermalization.

$G_{\mu\nu}^{+-\,[1]}(t,t';t_{\rm ob})$ and $G_{\mu\nu}^{-+\,[1]}(t,t';t_{\rm ob})$ for low temperatures can be given by

$$G_{\mu\nu}^{+-\,[1]}(t,t';t_{\rm ob})\simeq\mp i\hbar\lim_{\tau\to t_{\rm ob}-0}\theta(\tau-t)\lim_{\tau'\to t_{\rm ob}-0}\theta(\tau'-t')\times\sum_{\lambda}G_{\mu\lambda}^{++}(t,\tau;t_{\rm ob})G_{\lambda\mu}^{--}(\tau',t';t_{\rm ob}), \tag{23}$$

$$G_{\mu\nu}^{-+\,[1]}(t,t';t_{\rm ob})\simeq i\hbar\lim_{\tau\to t_{\rm ob}-0}\theta(\tau-t)\lim_{\tau'\to t_{\rm ob}-0}\theta(\tau'-t')\times\sum_{\lambda}G_{\mu\lambda}^{--}(t,\tau;t_{\rm ob})G_{\lambda\mu}^{++}(\tau',t';t_{\rm ob}). \tag{24}$$

These represent processes in which a particle excited at t (forward branch) or t' (backward branch) is scattered until $t_{\rm ob}$ and hence the density of the particle decreases as a function of $t_{\rm ob}$. The $t_{\rm ob}$ dependence of these Green functions shows that combination of the intrabranch and interbranch Green functions does *not* give the retarded and advanced Green functions, and the canonical transform of the Keldysh Green functions (the Keldysh rotation)[13,14,27] is available only for large $t_{\rm ob}$ at which the system is in the metastable state.

$G_{\mu\nu}^{+-\,[2]}(t,t';t_{\rm ob})$ and $G_{\mu\nu}^{-+\,[2]}(t,t';t_{\rm ob})$ within typical second-order diagrams with respect to V shown in Fig. 3 are given by

$$\begin{aligned}G_{\mu\nu}^{+-\,[2]}(t,t';t_{\rm ob})=&\mp(i\hbar)^2\sum_{\alpha}\sum_{\beta}\sum_{\gamma}[V_{\beta\gamma/\mu\alpha}V_{\alpha\mu/\gamma\beta}\\&\mp V_{\beta\gamma/\mu\alpha}V_{\alpha\mu/\beta\gamma}]\\&\times\int_{\infty}^{-\infty}d\tau'\int_{-\infty}^{\infty}d\tau\,G_{\mu\mu}^{++}(t,\tau;t_{\rm ob})\\&\times G_{\nu\nu}^{--}(\tau',t';t_{\rm ob})G_{\alpha\alpha}^{-+}(\tau',\tau;t_{\rm ob})\\&\times G_{\beta\beta}^{+-}(\tau,\tau';t_{\rm ob})G_{\gamma\gamma}^{+-}(\tau,\tau';t_{\rm ob}),\end{aligned} \tag{25}$$

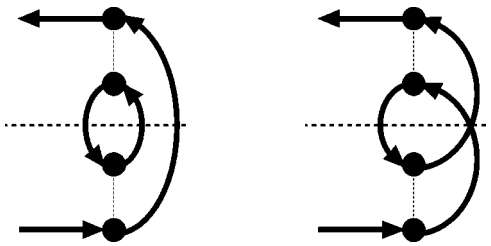

FIG. 3. Typical second-order diagrams for $G^{+-\,[2]}$ with respect to two-body interactions V denoted by dotted lines. The meanings of the symbols are the same with those in Fig. 1 (the Keldysh contour is omitted). The diagrams for $G^{-+\,[2]}$ are obtained by reversing the direction of the arrows.

$$\begin{aligned}G_{\mu\nu}^{-+\,[2]}(t,t';t_{\rm ob})=&\mp(i\hbar)^2\sum_{\alpha}\sum_{\beta}\sum_{\gamma}[V_{\gamma\mu/\beta\alpha}V_{\alpha\beta/\mu\gamma}\\&\mp V_{\gamma\mu/\beta\alpha}V_{\beta\alpha/\mu\gamma}]\\&\times\int_{\infty}^{-\infty}d\tau'\int_{-\infty}^{\infty}d\tau\,G_{\mu\mu}^{--}(t,\tau;t_{\rm ob})\\&\times G_{\nu\nu}^{++}(\tau',t';t_{\rm ob})G_{\alpha\alpha}^{-+}(\tau',\tau;t_{\rm ob})\\&\times G_{\beta\beta}^{-+}(\tau',\tau;t_{\rm ob})G_{\gamma\gamma}^{+-}(\tau,\tau';t_{\rm ob}),\end{aligned} \tag{26}$$

where the summations are taken over secondary quasiparticle states. These represent processes in which an original particle in $|\mu\rangle$ (forward branch) or $|\nu\rangle$ (backward branch) is inelastically scattered and hence three secondary particles are excited into $|\alpha\rangle$, $|\beta\rangle$ and $|\gamma\rangle$. Thus energies of the secondary particles dissipate toward the thermal equilibrium by repeating such processes, as we can express by high-order terms of $G_{\mu\nu}^{+-\,[2]}(t,t';t_{\rm ob})$ and $G_{\mu\nu}^{-+\,[2]}(t,t';t_{\rm ob})$ with respect to V.

III. HOLE DYNAMICS AT METAL SURFACES

We apply the Green functions introduced in the previous section to 2PPE from metal surfaces. 2PPE spectra of clean noble metal (111) surfaces show peaks due to occupied Shockley surface states and unoccupied image-potential induced surface states.[29] When the surfaces are covered with adsorbates (molecules), the peaks observed in the spectra of the clean surfaces are weakened and peaks due to adsorbate-induced occupied and unoccupied states are observed.[30,31] In this section, we investigate the dynamics of a hole photoexcited in an occupied state $|q\rangle$ at the clean or adsorbate-covered surfaces by calculating $G_{qq}^{+-}(t,t';t_{\rm ob})$.

We focus on the effects of hole decay and electron thermalization due to inelastic electron-electron scattering. In the femtosecond electron dynamics in metals, the available phase space for elastic and quasielastic scattering (including electron-phonon scattering) can be smaller than that for the

inelastic scattering. Then, by ignoring elastic and quasielasticscattering for simplicity, intrabranch Green functions become independent of absolute times as given by

$$\begin{aligned} G_{\mu\mu}^{++}(t-t') &= -[G_{\mu\mu}^{--}(t'-t)]^* \\ &\simeq (i\hbar)^{-1}\{\theta(E_\mu - E_F)\theta(t-t')e^{(-iE_\mu-\Gamma_\mu)(t-t')/\hbar} \\ &\quad - \theta(E_F-E_\mu)\theta(t'-t)e^{(iE_\mu-\Gamma_\mu)(t'-t)/\hbar}\}, \end{aligned} \tag{27}$$

where $\Gamma_\mu=\hbar/2\tau_\mu$ is the inverse lifetime of a state $|\mu\rangle$ and E_F is the Fermi level. From Eqs. (23) and (25), G_{qq}^{+-} can be given by

$$\begin{aligned} G_{qq}^{+-[1]}(t_{ob}-t,t'-t_{ob}) &= -(i\hbar)^{-1}\theta(E_F-E_q)\theta(t_{ob}-t)\theta(t_{ob}-t') \\ &\quad \times e^{(iE_q-\Gamma_q)(t_{ob}-t)/\hbar}e^{(-iE_q-\Gamma_q)(t_{ob}-t')/\hbar}, \end{aligned} \tag{28}$$

$$\begin{aligned} G_{qq}^{+-[2]}(t_{ob}-t,t'-t_{ob}) = -(i\hbar)^{-1}\theta(E_F-E_q)\theta(t_{ob}-t)\theta(t_{ob}-t')\sum_{\alpha}^{unocc}\sum_{\beta}^{occ}\sum_{\gamma}^{occ}[V_{\beta\gamma/q\alpha}V_{\alpha q/\gamma\beta}-V_{\beta\gamma/q\alpha}V_{\alpha q/\beta\gamma}] \\ \times[(E_q+E_\alpha-E_\beta-E_\gamma)^2+(\Gamma_q-\Gamma_\alpha-\Gamma_\beta-\Gamma_\gamma)^2]^{-1} \\ \times\{e^{(iE_q-\Gamma_q)(t_{ob}-t)/\hbar}-e^{[i(E_\alpha-E_\beta-E_\gamma)-(\Gamma_\alpha+\Gamma_\beta+\Gamma_\gamma)](t_{ob}-t)/\hbar}\} \\ \times\{e^{(-iE_q-\Gamma_q)(t_{ob}-t')/\hbar}-e^{[-i(E_\alpha-E_\beta-E_\gamma)-(\Gamma_\alpha+\Gamma_\beta+\Gamma_\gamma)](t_{ob}-t')/\hbar}\}. \end{aligned} \tag{29}$$

Here, for simplicity, we substitute $G^{+-[1]}$ and $G^{-+[1]}$ for G^{+-} and G^{-+} in the integral of Eq. (25).

$G_{qq}^{+-}(t,t';t_{ob})$ contains information on both densities of secondary electrons and holes and correlation between quantum phases in the forward and backward branches. The dynamical change of electron and hole densities can be represented by the average absolute time $[(t_{ob}-t)+(t_{ob}-t')]/2$ dependence of $G_{qq}^{+-}(t,t';t_{ob})$. This is understood from the photoelectron density ρ_{ff} for instantaneous laser pulses. For example, when the electric fields of the laser pulses are given by a delta function $\delta(t)$ so that $W_{qk'}(t)$, $W_{kq}(t)\propto\delta(t)$ and $W_{k'f}(t)$, $W_{fk}(t)\propto\delta(t-t_d)$, we obtain

$$\rho_{ff}(t_{ob})\propto\theta(t_{ob})e^{-t_d/\tau_k}\theta(t_{ob}-t_d)G_{qq}^{+-}(t_{ob},-t_{ob}). \tag{30}$$

Here we assume for simplicity that the photoexcitation of an electron occurs within a three-level system consisting of $|q\rangle$, $|k\rangle$, and $|f\rangle$.

In order to analyze effects of hole decay and thermalization, we divide ρ_{ff} into contributions from $G_{qq}^{+-[1]}$ and $G_{qq}^{+-[2]}$, i.e., $\rho_{ff}=\rho_{ff}^{[1]}+\rho_{ff}^{[2]}$. By substituting Eq. (28) for Eq. (30), we obtain

$$\rho_{ff}^{[1]}(t_{ob})\propto\theta(t_d)e^{-t_d/\tau_k}\theta(t_{ob}-t_d)e^{-t_{ob}/\tau_q}. \tag{31}$$

This shows that the observation probability of an electron in $|f\rangle$ decreases as time t_{ob} passes because of phase decay due to the decay of a hole in $|q\rangle$ represented by the t_{ob} dependence of $G_{qq}^{+-[1]}$. Thus the densities of both the photoelectron and the hole decrease so that the electron density of the whole system is conserved. Since the response time of the detector (e.g., time-of-flight analyzer) is on the submicrosecond time scale,[32] the measured photoelectron intensity $I(t_d)$ will be proportional to the integral of Eq. (31) over t_{ob}:

$$I_f^{[1]}(t_d)\propto\int_{-\infty}^{\infty}dt_{ob}\rho_{ff}^{[1]}(t_{ob})\propto\theta(t_d)\exp[-t_d(\tau_k^{-1}+\tau_q^{-1})]. \tag{32}$$

Thus we see that the decrease of $I_f(t_d)$ mainly due to the electron decay in $|k\rangle$ can be accelerated by the hole decay in $|q\rangle$.

In order to investigate the effects of thermalization, we show the numerical results of $G_{qq}^{+-[2]}$ for a localized state $|q\rangle$ in Fig. 4. Here, for simplicity, $V_{\beta\gamma/q\alpha}V_{\alpha q/\gamma\beta}-V_{\beta\gamma/q\alpha}V_{\alpha q/\beta\gamma}$ in Eq. (29) is assumed to be constant and the

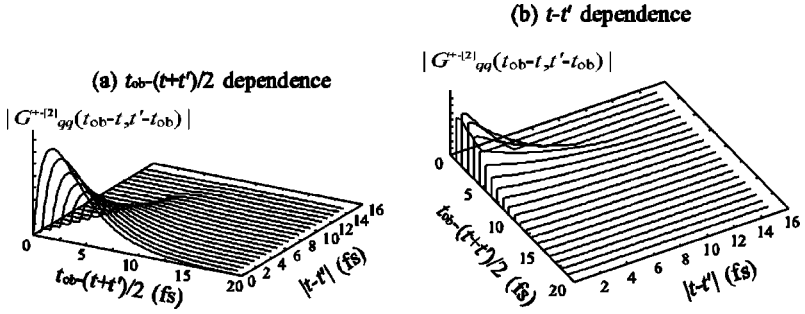

FIG. 4. Second-order term of the interbranch Green function $G_{qq}^{+-[2]}(t_{ob}-t,t'-t_{ob})$ with respect to V for an occupied state $|q\rangle$ with a lifetime $\tau_q=3$ fs plotted as a function of $t_{ob}-(t+t')/2$ and $t-t'$. (a) and (b) are plotted from different views by focusing on the $t_{ob}-(t+t')/2$ and $t-t'$ dependencies, respectively.

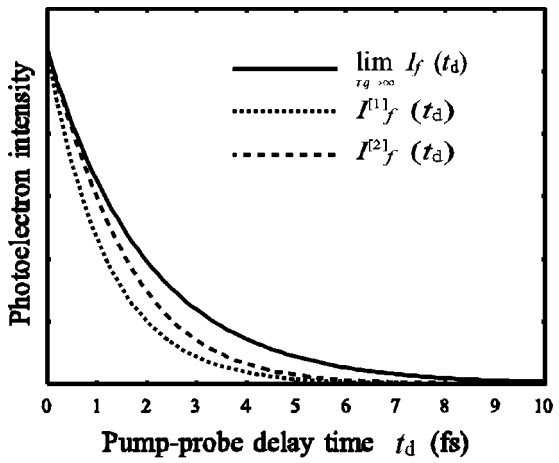

FIG. 5. Photoelectron intensity as a function of the pump-probe delay time for $\tau_k=2$ fs and $\tau_q=3$ fs. The dotted curve shows the term $I_f^{[1]}(t_d)$ representing the effects of hole decay, and the dashed curve shows the term $I_f^{[2]}(t_d)$ representing the effects of thermalization. The solid curve shows the photoelectron intensity $\lim_{\tau_q\to\infty} I_f(t_d)$ when the hole scattering is neglected. The values at $t_d=0$ are normalized to be the same.

lifetime of a bulk electron state with an energy E_μ is given by the Fermi liquid theory[33] as $\hbar/2\Gamma_\mu=(E_\mu-E_F)^{-2}\times 30$ fs [$\mu=\alpha$, β, and γ in Eq. (29)].[5] $G_{qq}^{+-\,[2]}$ becomes large when the scattering probability of the hole into the bulk is large so that the lifetime of the hole becomes short. Then, in the following calculation, we choose $\tau_q=3$ fs and $\tau_k=2$ fs which correspond to the shorter limits of the lifetimes of the highest occupied and lowest unoccupied molecular orbitals of NO/Cu(111),[31] respectively.

The $t_{ob}-(t+t')/2$ dependence of $G_{qq}^{+-\,[2]}(t_{ob}-t,t'-t_{ob})$ shows the time profile of densities of secondary electrons and holes in the bulk. When $t_{ob}-(t+t')/2=0$, the hole is localized at $|q\rangle$ and hence $G_{qq}^{+-\,[2]}(0,0)=0$. Then hole transfer from $|q\rangle$ occurs within τ_q due to inelastic scattering of the hole so that the densities of secondary electrons and holes in the bulk increase. Finally the electrons and holes decay due to inelastic scattering.

In Fig. 5, we show the numerical results of $I_f^{[2]}(t_d)\propto\int_{-\infty}^{\infty}dt_{ob}\rho_{ff}^{[2]}(t_{ob})$ with $I_f^{[1]}(t_d)$ and $\lim_{\tau_q\to\infty}I_f(t_d)\propto\exp(-t_d/\tau_k)$ for reference. For $t_d<\tau_q=3$ fs, $I_f^{[2]}$ decreases more slowly than $I_f^{[1]}$ since the rate of hole transfer from $|q\rangle$ to the bulk due to inelastic scattering is superior to the decay rate of the secondary electrons and holes in the bulk. For long t_{ob}, $I_f^{[2]}(t_d)$ decreases faster so that $I_f^{[2]}(t_d)$ exhibits a nonexponential behavior which can affect dephasing times estimated by phenomenological analysis of experimental data.

Here, we go back to Fig. 4 in order to focus on the $t-t'$ dependence of $G_{qq}^{+-\,[2]}(t_{ob}-t,t'-t_{ob})$, which shows the quantum phase correlation. Inelastic scattering of the hole in $|q\rangle$ causes excitation of secondary electrons and holes in various bulk states. The electrons and holes excited into states far from the Fermi level decay rapidly because of the large available phase space of inelastic electron-electron scattering. Thus the phase correlation in the short time scale is lost rapidly [see $G_{qq}^{+-\,[2]}(t_{ob}-t,t'-t_{ob})$ for $t_{ob}-(t+t')/2<5$ fs and $t-t'<5$ fs]. Consequently, in the long-time scale, only electrons and holes in the vicinity of the Fermi level remain in the bulk. This accounts for the gradual decrease of $G_{qq}^{+-\,[2]}(t_{ob}-t,t'-t_{ob})$ for $t_{ob}-(t+t')/2>5$ fs and $t-t'>5$ fs.

We show in the following that the $t-t'$ dependence of $G_{qq}^{+-\,[2]}(t_{ob}-t,t'-t_{ob})$ is directly related to the dephasing terms in Liouville–von Neumann equations (from which we obtain optical Bloch equations within the rotating-wave approximation[9]) for an open three-level system:

$$i\hbar\frac{\partial\rho^{B}_{\mu\nu}(t)}{\partial t}=[H_0+W(t),\rho^{B}(t)]_{\mu\nu}-i\Gamma_{\mu\nu}\rho^{B}_{\mu\nu}(t)$$
$$(\mu,\ \nu=f,\ k,\ q \text{ except for } \mu=\nu=q), \tag{33}$$

and $\rho^{B}_{qq}(t)=1$. Here the diagonal elements of Γ give the inverse lifetimes by $\Gamma_{ff}=0$ and $\Gamma_{kk}=2\Gamma_k$. The off-diagonal elements give the inverse dephasing times by $\Gamma_{kf}=\Gamma_{fk}=\Gamma_k$, $\Gamma_{qk}=\Gamma_{kq}=\Gamma_k+\Gamma_q+\overline{\Gamma}$, and $\Gamma_{qf}=\Gamma_{fq}=\Gamma_q+\overline{\Gamma}$, where $\overline{\Gamma}$ is an inverse pure dephasing time.[34] By using Eq. (27), we obtain the photoelectron density within the fourth order with respect to W:

$$\begin{aligned}\rho^{B}_{ff}(t_{ob})=-i\hbar\int_{\infty}^{-\infty}dt_1'\int_{\infty}^{-\infty}dt_2'\int_{-\infty}^{\infty}dt_2\int_{-\infty}^{\infty}dt_1\\ \times\theta(t_{ob}-t_2')\theta(t_2'-t_1')\theta(t_{ob}-t_2)\theta(t_2-t_1)\\ \times W_{qk}(t_1')W_{kf}(t_2')W_{fk}(t_2)W_{kq}(t_1)\\ \times G_{ff}^{++}(t_{ob}-t_2)G_{kk}^{++}(t_2-t_1)\overline{G}_{qq}^{+-}(t_1-t_1')\\ \times G_{kk}^{--}(t_1'-t_2')G_{ff}^{--}(t_2'-t_{ob}),\end{aligned} \tag{34}$$

where

$$\overline{G}_{qq}^{+-}(t-t')=-(i\hbar)^{-1}\theta(E_F-E_q)[\exp-iE_q(t-t')/\hbar-(\Gamma_q+\overline{\Gamma})|t-t'|/\hbar]. \tag{35}$$

By comparing with the numerical results of $G_{qq}^{+-}(t,t';t_{ob})$, we see that $\overline{G}_{qq}^{+-}(t-t')$ represents the phase correlation between two times t and t' by assuming a mean dephasing time $\hbar[\Gamma_q+\overline{\Gamma}]^{-1}$ instead of considering the nonexponential behavior of $G_{qq}^{+-}(t,t';t_{ob})$ shown in Fig. 4(b). The photoelectron intensity as a function of t_d (correlation trace) becomes narrower when the mean dephasing time is shortened.[12,35] Since $\overline{G}_{qq}^{+-}(t-t')$ is independent of t_{ob}, $\rho^{B}_{ff}(t_{ob})$ is not affected by the dynamical change of the density of secondary electrons and holes in the bulk. However, referring to the results in Fig. 5, we see that both the $t_{ob}-(t+t')/2$ and $t-t'$ dependencies of $G_{qq}^{+-}(t_{ob}-t,t'-t_{ob})$ can account for the narrowing of the correlation trace.

When scattering probability of the photoexcited hole in $|q\rangle$ is small so that τ_q is long, $G_{qq}^{+-\,[1]}$ becomes the main term of G_{qq}^{+-}. In this case, the correlation trace can be affected by τ_q so that the effective lifetime measured at an

energy position $E_k+E_{\rm probe}$, where $E_{\rm probe}$, the probe photon energy, depends on the pump photon energy $E_{\rm pump}$. It is known that effective lifetimes of bulk states in metals exhibit $E_{\rm pump}$ dependence.[5,36] The experimental results were once explained by considering effects of cascade and Auger processes,[4,12,35–38] however, recent experimental results suggest that other mechanisms can be involved in the 2PPE process.[6] We can deduce that the hole decay affects the dynamical change of the probability of cascade and Auger processes as well as the photoelectron density shown in Eq. (32). This will give a hint for solving the problem about the effective lifetimes.

When the scattering probability is large so that τ_q is short, $G_{qq}^{+-\,[2]}$ becomes the main term. In this case, the correlation trace can be affected by the lifetimes of secondary electrons and holes in the vicinity of $E_{\rm F}$. When the temperature of the metal is finite, the lifetimes of the electrons and holes are shortened because of scattering by thermally fluctuating electrons and phonons[33] so that the mean dephasing time can be shortened due to electron thermalization whereas it is usually considered that temperature dependence of dephasing times is due to electron-phonon interactions.[5]

IV. 1PPE SPECTRA

When the pulse duration becomes long so that the energy width of the light becomes narrow, the energy spectra of photoelectrons reflect the electronic density of states of the sample materials. The energy spectra can be measured by 1PPE as well as 2PPE.[19,25] There are many theoretical studies of 1PPE from solids including metals by Green-function methods (or by other methods based on the perturbation theory).[18,20–24] Most of the theories can be approximately classified into two by methods of countermeasure to the problem of the absolute-time dependence of the Green functions: (i) avoid the problem by calculating the transition matrix without using nonequilibrium Green functions;[23,24] (ii) ignore the problem and employ the spectral theorem.[18–22,25] By using the Green functions introduced in this paper, the systematic method beyond (i) and (ii) becomes available. In this section, we show the relation of methods (i) and (ii) with the method introduced in this paper.

Usually, the 1PPE spectra can be obtained by assuming static light irradiation within the rotating-wave approximation:

$$W_{fq}(t)=[W_{qf}(t)]^*=W_{fq}e^{-iE_{\rm p}t/\hbar}, \tag{36}$$

where $E_{\rm p}$ is the photon energy. When applying the Green functions introduced in this paper, the 1PPE spectrum is obtained as

$$I^{\rm 1P}[E]\propto\rho_{ff}[E], \tag{37}$$

$$\rho_{ff}[E]=\frac{1}{i\hbar}|W_{fq}|^2G_{qq}^{+-}[E-E_{\rm p}-i\xi,E-E_{\rm p}+i\xi], \tag{38}$$

for $\xi\rightarrow+0$. Here the Fourier transform of $G^{+-}(t_{\rm ob}-t,t'-t_{\rm ob})$ is defined by

$$G^{+-}[E,E']=\int_{-\infty}^{\infty}{\rm d}\tau\int_{-\infty}^{\infty}{\rm d}\tau'\,e^{-i(E\tau+E'\tau')/\hbar}G^{+-}(\tau,\tau'). \tag{39}$$

By using Eqs. (28) and (29), we obtain

$$\rho_{ff}[E]=|W_{fq}|^2[(E-E_{\rm p}-E_q)^2+\Gamma_q^2]^{-1}\times\{1+i\hbar\Sigma_{qq}^{+-}[E-E_{\rm p}-i\xi,E-E_{\rm p}+i\xi]\}, \tag{40}$$

$$\Sigma_{qq}^{+-}[E,E']=\frac{1}{i\hbar}\sum_{\alpha}^{\rm unocc}\sum_{\beta}^{\rm occ}\sum_{\gamma}^{\rm occ}[V_{\beta\gamma/q\alpha}V_{\alpha q/\gamma\beta}-V_{\beta\gamma/q\alpha}V_{\alpha q/\beta\gamma}]\times[E+E_\alpha-E_\beta-E_\gamma-i(\Gamma_\alpha+\Gamma_\beta+\Gamma_\gamma)]^{-1}\times[E'+E_\alpha-E_\beta-E_\gamma+i(\Gamma_\alpha+\Gamma_\beta+\Gamma_\gamma)]^{-1}. \tag{41}$$

The first and second terms in the brace in Eq. (40) are obtained from $G_{qq}^{+-\,[1]}$ and $G_{qq}^{+-\,[2]}$, respectively. The first Lorentzian $[(E-E_{\rm p}-E_q)^2+\Gamma_q^2]^{-1}$ shows the density of states in $|q\rangle$ given by $|G_{qq}^{++}[E-E_{\rm p}+i\xi]|^2$, where $G_{\mu\mu}^{++}[E]$ is the Fourier transform of $G_{\mu\mu}^{++}(t-t')$ given by Eq. (27). The second Lorentzian $[(E-E_{\rm p}+E_\alpha-E_\beta-E_\gamma)^2-(\Gamma_\alpha+\Gamma_\beta+\Gamma_\gamma)^2]^{-1}$ shows the density of states in the bulk given by $|G_{\alpha\alpha}^{++}[E-E_{\rm p}+i\xi]*G_{\beta\beta}^{++}[E-E_{\rm p}+i\xi]*G_{\gamma\gamma}^{++}[E-E_{\rm p}+i\xi]|^2$, where '$*$' denotes convolution.

The spectra obtained by method (i) include parts corresponding to the squared absolute values of G^{++} similar to Eq. (40).[23,24] Thus this method will be partially equivalent to the method introduced in this paper although systematic investigation of many-body effects by diagrammatic technique will be difficult.

The spectra obtained by method (ii) are approximately proportional to the imaginary parts of the retarded Green functions.[18–22,25] In the spectral theorem, the Green functions are assumed to be functions of the relative times and then complicated many-body effects can be taken into account in the similar way to equilibrium Green functions. From Eq. (34), method (ii) will be partially equivalent to the density-matrix method. Therefore the spectra obtained by method (ii) will be related with the second term of Eq. (40) as seen from the formulas of the retarded Green functions usually given by ${\rm Im}G^{\rm r}[E]={\rm Im}\Sigma[E]/[(E-{\rm Re}\Sigma[E])^2+({\rm Im}\Sigma[E])^2]^{-1}$, where $\Sigma[E]$ is the self-energy function.

The Fourier transform of the Green functions introduced in this paper are functions of two energies corresponding to the time evolution in the forward and backward branches while those used in method (ii) are functions of one energy. The importance of distinction between the two energies will be understood from Eq. (4) which can be rewritten as a sum of squared absolute values of multiple convolutions. Therefore, when more complicated dynamics is involved, the ''for-

tunate'' agreement between method (ii) and the method introduced in this paper as obtained for the 1PPE spectra will not be guaranteed.

V. CONCLUSIONS

In conclusion, we have introduced nonequilibrium Green functions depending on the observation time so that we can investigate the dynamics of secondary particles which remain in the final state. The observation time dependence of the Green functions represents the effects of phase decay due to scattering of the secondary particles. By applying the Green functions to 2PPE from a metal surface, we showed that photoexcited hole decay shortens effective lifetimes and electron thermalization affects pure dephasing times. The present theory will be used as an entrance into microscopic analysis of pure dephasing times at metal surfaces.

The absolute-time dependence of the Green functions introduced in this paper is derived from the pure quantum statistics without any deduction from classical theories[14] nor any additional condition, e.g., the generalized Kadanoff-Baym ansatz.[15] Intensive investigation using the Green functions introduced in this paper is expected to contribute to clarification of microscopic mechanisms of both relaxation and dephasing in general systems as well as metal surfaces.

ACKNOWLEDGMENTS

One of the authors (M.S.) acknowledges the support by the Special Postdoctoral Researchers Program of RIKEN. This work was partly supported by the Ministry of Education, Culture, Sports, Science and Technology of Japan, through their Grant-in-Aid for COE Research (Grant No. 10CE2004), Scientific Research (Grant Nos. 11640375, and 13650026) programs, by the New Energy and Industrial Technology Development Organization (NEDO), through their Materials and Nanotechnology program, and by the Japan Science and Technology Corporation (JST), through their Research and Development Applying Advanced Computational Science and Technology program.

*Electronic address: dmsakaue@postman.riken.go.jp
†URL: http://www.dyn.ap.eng.osaka-u.ac.jp

[1] G. A. Burdick, Phys. Rev. **129**, 138 (1963).
[2] P. M. Echenique, J. M. Pitarke, E. V. Chulkov, and A. Rubio, Chem. Phys. **251**, 1 (2000).
[3] M. Weinelt, Surf. Sci. **482-485**, 519 (2001).
[4] E. Knoesel, A. Hotzel, and M. Wolf, Phys. Rev. B **57**, 12 812 (1998).
[5] H. Petek and S. Ogawa, Prog. Surf. Sci. **56**, 239 (1997).
[6] H. Petek, H. Nagano, M. J. Weida, and S. Ogawa, Chem. Phys. **251**, 71 (2000).
[7] A. Fukui, H. Kasai, H. Nakanishi, and A. Okiji, J. Phys. Soc. Jpn. **70**, 29 (2001).
[8] J. P. Gauyacq, A. G. Borisov, and G. Raşeev, Surf. Sci. **490**, 99 (2001).
[9] R. Loudon, *The Quantum Theory of Light*, 2nd ed. (Oxford University Press, New York, 1983).
[10] *Optical Properties of Solids*, edited by F. Abelés (North-Holland, Amsterdam,1972).
[11] T. Mii and H. Ueba, J. Lumin. **87-89**, 898 (2000).
[12] M. Sakaue, H. Kasai, and A. Okiji, J. Phys. Soc. Jpn. **39**, 4380 (2000).
[13] L. V. Keldysh, Zh. Éksp. Teor. Fiz. **47**, 1945 (1964) [Sov. Phys. JETP **20**, 1018 (1965)].
[14] A. M. Zagoskin, *Quantum Theory of Many-Body Systems* (Springer-Verlag, New York, 1998).
[15] P. Lipavský, V. Špička, and B. Velický, Phys. Rev. B **34**, 6933 (1986).
[16] L. Bányai, Q. T. Vu, B. Mieck, and H. Haug, Phys. Rev. Lett. **81**, 882 (1998).
[17] Y. Kurokawa and T. Takemori, J. Lumin. **87-89**, 1220 (2000).
[18] N. Fominykh, J. Henk, J. Berakdar, P. Bruno, H. Gollisch, and R. Feder, Solid State Commun. **113**, 665 (2000).
[19] S. Hüfner, R. Claessen, F. Reinert, T. Straub, V. N. Strocov, and P. Steiner, J. Electron Spectrosc. Relat. Phenom. **100**, 191 (1999).
[20] C. Meyer, J. Braun, G. Borstel, M. Potthoff, T. Wegner, and W. Nolting, Surf. Sci. **454–456**, 447 (2000).
[21] M. Milun, P. Pervan, and D. P. Woodruff, Rep. Prog. Phys. **65**, 99 (2002).
[22] T. Fujikawa and H. Arai, J. Electron Spectrosc. Relat. Phenom. **123**, 19 (2002).
[23] J. C. Parlebas, A. Kotani, and J. Kanamori, J. Phys. Soc. Jpn. **51**, 124 (1982).
[24] V. M. Tapilin, Surf. Sci. **383**, 226 (1997).
[25] R. Matzdorf, Surf. Sci. Rep. **30**, 153 (1998).
[26] M. Sakaue, H. Kasai, and A. Okiji, J. Phys. Soc. Jpn. **68**, 720 (1999).
[27] C. Niu, D. L. Lin, and T.-H. Lin, J. Phys. C **11**, 1511 (1999).
[28] M. Sakaue, T. Munakata, H. Kasai, and A. Okiji, J. Phys. Soc. Jpn. **71**, 872 (2002).
[29] W. Steinmann, Appl. Phys. A: Solids Surf. **49**, 365 (1989).
[30] K. Ishioka, C. Gahl, and M. Wolf, Surf. Sci. **454–456**, 73 (2000).
[31] T. Munakata, J. Electron Spectrosc. Relat. Phenom. **76**, 371 (1995).
[32] J. T. Yates, Jr., *Experimental Innovations in Surface Science: A Guide to Practical Laboratory Methods and Instruments* (Springer-Verlag, New York, 1998).
[33] A. A. Abrikosov, L. P. Gor'kov, and I. Y. Dzyaloshinskii, *Quantum Field Theoretical Methods in Statistical Physics*, 2nd ed. (Pergamon, New York, 1965).
[34] When we consider another pure dephasing time in Γ_{kf}, we can obtain results including a decay function of $|t_2-t_2'|$ in Eq. (34). This function concerns with the part $G_{kk}^{+-}(t_2,t_1;t_{\rm ob})G_{k'k'}^{-+}(t_1',t_2';t_{\rm ob})$ in Eq. (6).
[35] M. Sakaue, H. Kasai, and A. Okiji, J. Phys. Soc. Jpn. **69**, 160 (2000).
[36] R. Knorren, K. H. Bennemann, R. Burgermeister, and M. Aeschlimann, Phys. Rev. B **61**, 9427 (2000).
[37] M. Sakaue, H. Kasai, and A. Okiji, Appl. Surf. Sci. **169–170**, 68 (2001).
[38] H. Kasai, W. A. Dino, and A. Okiji, Surf. Sci. Rep. **43**, 1 (2001).